the plant journal

SEB SOCIETY FOR EXPERIMENTAL BIOLOGY

The Plant Journal (2025) **122,** e70186 doi: 10.1111/tpj.70186

GERMIN3 regulates tuber initiation and axillary bud activation by facilitating plasmodesmatal gating

Raymond Campbell[1], Graham Cowan[1], Bernhard Wurzinger[2,3], Laurence J. M. Ducreux[1], Jimmy Dessoly[1], Wenbin Guo[4,†], Runxuan Zhang[4], Jenny A. Morris[1], Pete Hedley[1], Vanessa Wahl[1], Mark A. Taylor[1] and Robert D. Hancock[1,*]

[1]*Cell and Molecular Sciences, The James Hutton Institute, Invergowrie, Dundee DD2 5DA, UK,*
[2]*Department of Functional and Evolutionary Ecology, University of Vienna, Vienna, Austria,*
[3]*Department of Applied Genetics and Cell Biology, BOKU University, Vienna, Austria, and*
[4]*Information and Computational Sciences, The James Hutton Institute, Invergowrie, Dundee DD2 5DA, UK*

Received 19 December 2024; revised 9 April 2025; accepted 15 April 2025.
*For correspondence (e-mail rob.hancock@hutton.ac.uk).
[†]Present address: Higentech Breeding Innovation (ZheJiang) Co. Ltd., Wanyang Innovation Park, Bihu Town, Liandu District, Lishui, Zhejiang, China

SUMMARY

***GERMIN3* has previously been identified as a target of the tuberigen activation complex, suggesting a function in potato tuberisation, but its role is presently unknown. In the present study, we analysed morphological, agronomic and molecular phenotypes of GERMIN3 transgenic lines in *Solanum tuberosum* ssp. *andigena* and in the tuberosum cultivar Desiree. *GERMIN3* over-expressing lines of *S. tuberosum* ssp. *andigena* exhibited increased tuber yields and enhanced tuber numbers. Post-harvest tuber sprouting exhibited greater bud activation with increased numbers of sprouts. Axillary buds were also activated in aerial tissues of mature plants, resulting in increased stem branching. Similar results were observed in the commercial cultivar Desiree. Over-expression of *GERMIN3* had no impact on the expression of *SP6A*, a positive regulator of tuberisation, or *TFL1B*, a negative regulator. The GERMIN3 protein localised to the endoplasmic reticulum, and transient expression in *N. benthamiana* leaves resulted in plasmodesmatal gating, allowing intercellular transport of GFP-tagged sporamin independent of GERMIN3 oxalate oxidase activity. We propose that GERMIN3 affects tuberisation and other developmental processes by facilitating meristem activation. This identifies GERMIN3 as a novel protein associated with control of plasmodesmatal transport and supports the importance of plasmodesmatal gating in the regulation of key potato developmental processes.**

Keywords: GERMIN-like proteins, meristems, plant development, plasmodesmata, *Solanum tuberosum* (potato), tuberisation.

INTRODUCTION

GERMINs and GERMIN-like proteins (GLPs) are water-soluble glycoproteins widely found in plants (Dunwell et al., 2008). GLPs belong to large gene families, often found as multiple copies at specific chromosomal loci (Ilyas et al., 2020; Zaynab et al., 2022). GERMINs and GLPs have been implicated in many biological processes, including roles in signalling cascades associated with responses to both biotic and abiotic stresses (Berna & Bernier, 1999; Davidosn et al., 2009; Gangadhar et al., 2021). This is in part mediated via the fact that many of them have oxalate oxidase or superoxide dismutase activity (Lane et al., 1993; Woo et al., 2000) and are reported to participate in plant responses involving hydrogen peroxide (H_2O_2) production. In potato, a GLP is associated with heat tolerance based on the enhanced *in vitro* growth performance of over-expressing (OE) transgenic lines subjected to heat stress scenarios (Gangadhar et al., 2021). This tolerance was attributed to the activation of transcripts encoding antioxidant enzymes and stress-responsive heat shock proteins caused by enhanced levels of H_2O_2 in the OE lines. In Arabidopsis, other GLP proteins are located in the plasmodesmata (PD) where they appear to have a role in the control of cell-to-cell trafficking (Ham et al., 2012).

During potato tuber development, prior to tuber induction, phloem unloading in elongating stolons is apoplastic both in the region of the apical meristem and in the subapical region (Viola et al., 2001). As the sub-apex swells during early tuberisation, induction of symplastic unloading (via PD) allows increased photoassimilate delivery, and division and expansion of parenchyma cells to create the tuber. Initiation of tuber swelling involves localised

changes in sugar-responsive gene expression as well as PD and phloem function (Viola et al., 2001), potentially allowing the unloading of phloem-mobile signalling molecules, but the triggers for, and orchestration of, these events are not currently understood.

Throughout tuber development, axillary meristems remain symplastically isolated, maintaining a tightly controlled cellular domain around the bud as dormancy is established, limiting substrate availability and necessitating the active transport of signalling compounds into the meristematic tissue. In sprouting tubers, dormancy break is associated with symplastic re-connection of the axillary meristem to the tuber phloem network, allowing the free diffusion of phloem-mobile signalling molecules and stored photoassimilates into the meristematic region (Viola et al., 2007). These observations strongly suggest that symplastic connectivity or isolation is a key mechanism controlling stolon/tuber bud meristem activity by regulating the supply of substrates and signalling compounds. Control of symplastic continuity is regulated by PD, which connect cells and tissues into symplastic domains. Despite their importance, the molecular properties of PD are largely elusive or speculative (Han et al., 2019), but these structures are a likely control point for tissue function and tuber life-cycle regulation.

A complex termed the tuberigen activation complex (TAC) comprising SP6A, 14-3-3s, and the group A bZIP transcription factor FLOWERING LOCUS D–LIKE 1 has recently been identified (Teo et al., 2017). The TAC has a regulatory role in tuber initiation, acting in an analogous manner to the florigen activation complex for flowering. We have recently identified a *TFL1* gene (designated *CEN/TFL1B*) that encodes a protein thought to compete with SP6A in the TAC. Binding of TFL1B in this complex results in an inactive TAC complex (Zhang et al., 2020), RNAi-*TFL1B* lines tuberise earlier than wild-type (WT) and *35S::TFL1B* lines have delayed tuberisation.

In order to identify potential TAC targets, we carried out transcriptomic analysis of non-swelling stolons from WT compared with RNAi lines silenced for *TFL1B*. As the RNAi-*TFL1B* lines tuberise earlier, the non-swelling stolons from this genotype are primed for tuberisation and so a comparison with WT should reveal genes expressed early in tuber initiation. As well as many of the known genes which showed upregulation at the onset of tuberisation (Hancock et al., 2014; Park et al., 2022), several transcripts encoding GERMIN proteins were identified. Transcripts annotated as *GERMIN3*, *4* and *12* are expressed at levels between 200- and 700-fold higher in the stolons from RNAi-*TFL1B* lines than in those from controls. The most strongly upregulated *GERMIN* (*GERMIN3*) was directly transcriptionally regulated by the TAC complex (Zhang et al., 2020).

In view of the identification of *GERMIN3* as a direct target of the TAC, we wished to investigate the role of the protein in potato. We demonstrate that over-expression of *GERMIN3* is associated with accelerated tuberisation and higher tuber yield. Moreover, OE lines exhibit a meristem activation phenotype with increases in post-harvest tuber sprouting and the development of more highly branched stems as axillary buds are activated. We show that the GFP-tagged GERMIN3 protein localises to the ER and regulates cell-to-cell movement of protein via the PD.

RESULTS

Over-expression of GERMIN3 impacts meristem activation processes in potato

In order to probe the function of GERMIN3, transgenic lines were produced in *Solanum tuberosum* ssp. *andigena*, an obligate short-day potato (Jackson et al., 1996). The *GERMIN3* sequence used was from the Phureja double monoploid DM 1–3515 R44 (based on transcript number PGSC0003DMT400046995, 99.8% sequence similar to Soltu.DM.01G041670, available at Spud DB [http://spuddb.uga.edu/]) and transgene expression was driven by a constitutive *35S* Cauliflower Mosaic Virus promoter. Twenty-six independent transgenic lines were screened for *GERMIN3* expression in leaves by qRT-PCR from tissue culture plantlets (Figure 1a). Sixteen lines exhibiting varying levels of *GERMIN3* expression were grown as described, and tuber yield was measured 47 days following sub-culturing. A strong and highly significant linear correlation between either leaf (Figure 1b) or stolon (Figure 1c) *GERMIN3* transcript abundance and tuber yield was observed. Five lines exhibiting high *GERMIN3* expression (lines 66, 69, 79, 89 and 91) were therefore selected for further analysis (Figure 1a). Although line 22 exhibited high abundance of *GERMIN3* transcripts, it grew poorly under tissue culture and glasshouse conditions and so was excluded from further analysis. In the selected lines, tuber yield was measured at two harvest points (47 and 93 days) with four out of the five OE lines exhibiting higher yield than WT plants (Figure 2a,c; Figure S1). Similarly, at the earlier time point, three of the four transgenic lines exhibited a higher tuber number (Figure 2b) although after 93 days, the tuber number phenotype was no longer apparent (Figure 2d). These data suggest that over-expression of *GERMIN3* advances the date of tuber initiation and facilitates tuber bulking.

A similar phenotype was observed in *S. tuberosum* cv. Desiree plants in which *GERMIN3* was expressed under 35S or the tuber-active *PATATIN* (*PAT*) promoter (Miroshnichenko et al., 2020) where two of three 35S and two of three *PAT* lines exhibited a significantly higher tuber yield 47 days after transfer to the glasshouse, which was maintained in one 35S line and both *PAT* lines after 73 days (Figure S2). Knockdown of *GERMIN3* using RNAi technology had little impact on tuber yield, with only one line

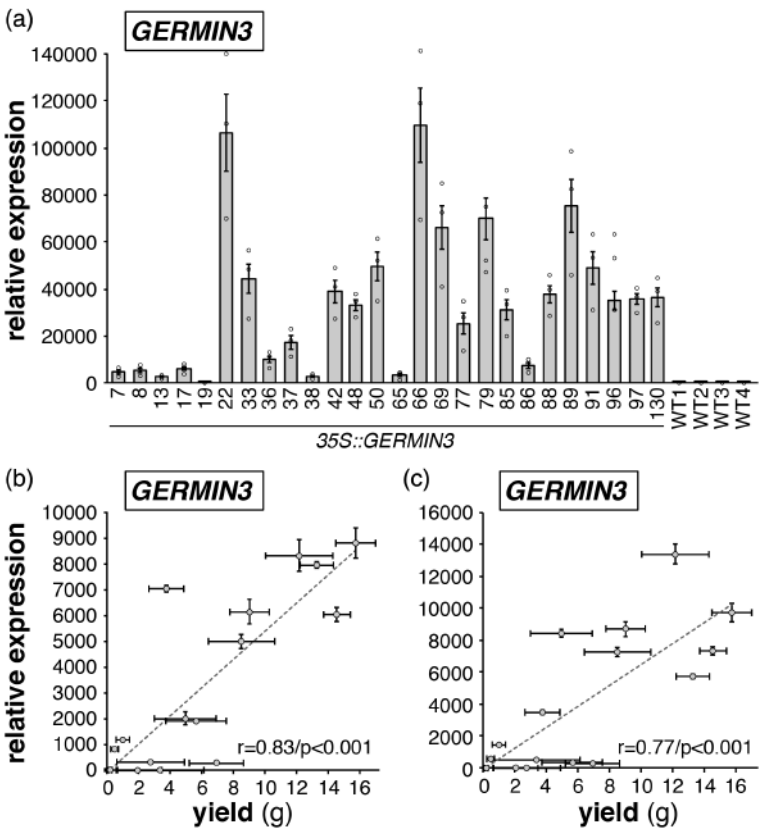

Figure 1. Relationship between GERMIN3 gene expression and tuber yield in GERMIN3 over-expressing (OE) *Solanum tuberosum* ssp. *andigena* transgenic lines.
Relative abundance of the *GERMIN3* transcript in tissue culture leaflets in 26 OE lines and *andigena* controls (wild-type) is indicated (a) showing the variation in transcript abundance between lines.
Sixteen lines were selected for further analysis and tuber yield was quantified 14 days after transfer to inductive short-day conditions and correlated against leaf (b) and stolon (c) *GERMIN3* transcript abundance. Expression levels were determined by RT-qPCR relative to the reference gene *StEF1α*. All data are represented as mean ± SE of three independent biological replicates and individual data points are presented in panel (a). The correlation coefficient (*r*) and statistical significance (*P*) of the correlation are indicated in panels (b, c).

showing a slight reduction after 73 days despite a reduction in transcript abundance of up to 80% (Figure S2).

The sprouting characteristics of tubers from the OE lines were compared with those of WT plants. Sprouting was monitored in tubers stored at 10°C for up to 160 days. While there was little difference in the time point when sprouting initiated between WT and transgenic lines (approximately 105 days), sprout number was significantly higher in four of the five *35S* lines relative to WT, indicating increased bud activity (Figure 3).

The OE lines also exhibited above-ground phenotypes, most notably a more highly branched growth pattern, in which the axillary buds, showing little or no outgrowth in WT plants, exhibited significant growth in the *35S* lines (Figure 4). The length of the stem derived from the axillary bud was measured in all nodes of the WT and OE lines 66 and 79 (Figure 4a). Significant axillary bud outgrowth was observed particularly between nodes 6 and 14. Internode length was also quantified, indicating that all lines exhibited longer nodes in the middle region of the plant, with OE lines (Figure 4b), particularly line 66, having longer nodes than WT plants in many cases, which led to an overall increase in plant height (Figure 4c). In addition to the axillary bud outgrowth in the OE lines that was not observed in WT (Figure 4d–f) we observed the growth of an organ resembling a stolon and an associated leaf in some nodes (Figure 4g). Taken together, these data indicate that the bud activation observed in tubers, which are modified subterranean stems, is also apparent in aerial stems.

Similar phenotypes were also observed in 'Desiree' plants expressing the *GERMIN3* construct under the *35S* promoter where axillary branches were typically more strongly developed (Figure S3a), internode lengths were altered (Figure S3b), and axillary bud outgrowth resulted in the production of stems, leaves and aerial stolons (Figure 3c–g).

The flowering phenotype of OE *andigena* lines was also altered, where *andigena* line 66 exhibited earlier flowering than WT lines after 56 days growth (Figure S4).

GERMIN3 is expressed in multiple organs of WT *S. tuberosum* ssp. *andigena* plants and is induced by tuberisation and starvation

The expression profile of *GERMIN3* in WT *S. tuberosum* ssp. *andigena* was determined by RT-qPCR analysis 14 days after transfer to inductive conditions when plants had stolons in multiple stages of development. A marked increase in transcript abundance was observed on transition from hooked to swelling stolons, and expression remained elevated through late swelling and early tuber development (Figure 5a). On the contrary, where stolons

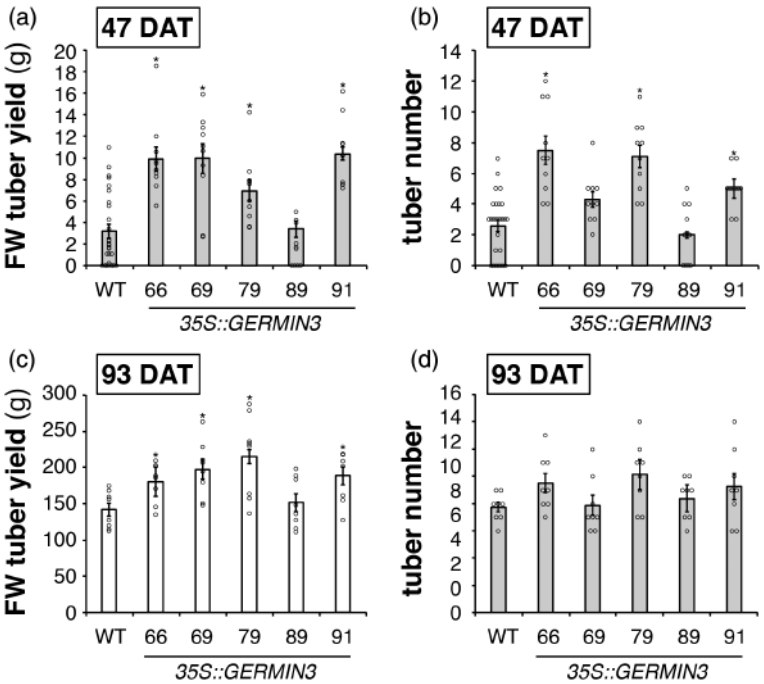

Figure 2. Tuber yield and number in wild-type and GERMIN3 over-expressing *Solanum tuberosum* subsp. *andigena* transgenic lines.
Tuber yield (FW) and number were measured in *35S::GERMIN3* lines and WT control. Plants were grown in pots under standard glasshouse conditions (18/15°C, 16 h daylength) for 35 days, then moved to a controlled environment (18/15°C) under short days (10 h daylength).
Plants were harvested at 47 (a, b) and 93 (c, d) days after planting, and tuber yield (a, c) and number (b, d) were recorded. All data are represented as means ± SE of 10 independent biological replicates at days 47 and six independent biological replicates at day 93, where individual data points are indicated. Asterisks denote values that were significantly different between transgenic lines and wild-type controls as determined by one-way ANOVA followed by Fisher's protected Least significant difference (LSD) test ($P < 0.05$).

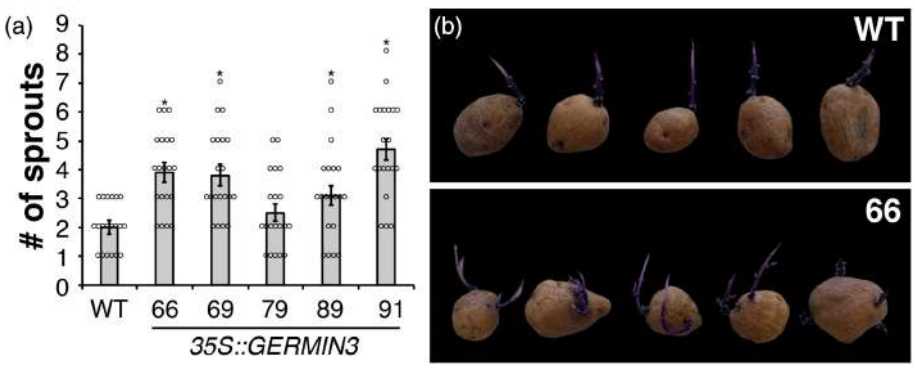

Figure 3. Number of sprouts recorded following tuber storage at 10°C in wild-type (WT) and GERMIN3 over-expressing (OE) *Solanum tuberosum* ssp. *andigena* lines.
Twenty tubers harvested from 10 replicate plants were stored at 10°C in the dark for 160 days, and tuber dormancy was monitored.
The number of individual tuber shoots with a length greater than 2 mm was counted and compared with ADG WT control (a). All data are represented as mean ± SE of 20 replicates (individual tubers, data points indicated). Asterisks denote values that were significantly different between transgenic lines and WT controls as determined by one-way ANOVA followed by Fisher's protected LSD test ($P < 0.05$).
The phenotypes of WT and OE line 66 are indicated in panel (b).

were exposed to light following breaking through the surface of the substrate, *GERMIN3* abundance was reduced.

Consistent with our observations regarding the aerial phenotype of *GERMIN3* OE lines, the gene was also expressed in the shoot apex, the stem between nodes and nodal regions of plants as well as in the leaf and roots (Figure 5b). Expression of the gene under the *35S* promoter significantly enhanced transcript abundance in all tissues tested, particularly in line 79 (Figure 5b).

RNA *in situ* hybridisation experiments supported our observation that *GERMIN3* expression was limited in uninduced stolons where we were unable to detect any signal (Figure 5c). Similarly, no staining was observed with a full-length *GERMIN3* antisense probe in 2-day-induced stolons. On the contrary, stage 4 swellings exhibited significant staining associated with the cortex and vascular tissue, supporting our RT-qPCR observations and indicating tissue-specific expression within the developing tuber.

Group A bZIP transcription factors have well established functions in driving developmental processes such as flowering and tuberisation, forming essential components of both the TAC (FDL1a/bZIP27) and the FAC (FD/bZIP14) (Abe et al., 2005; Teo et al., 2017). Moreover, previous work has demonstrated the capacity of multiple bZIPs to form complexes with 14-3-3 proteins and PEBPs (reviewed by Martignago et al., 2025). Therefore, to

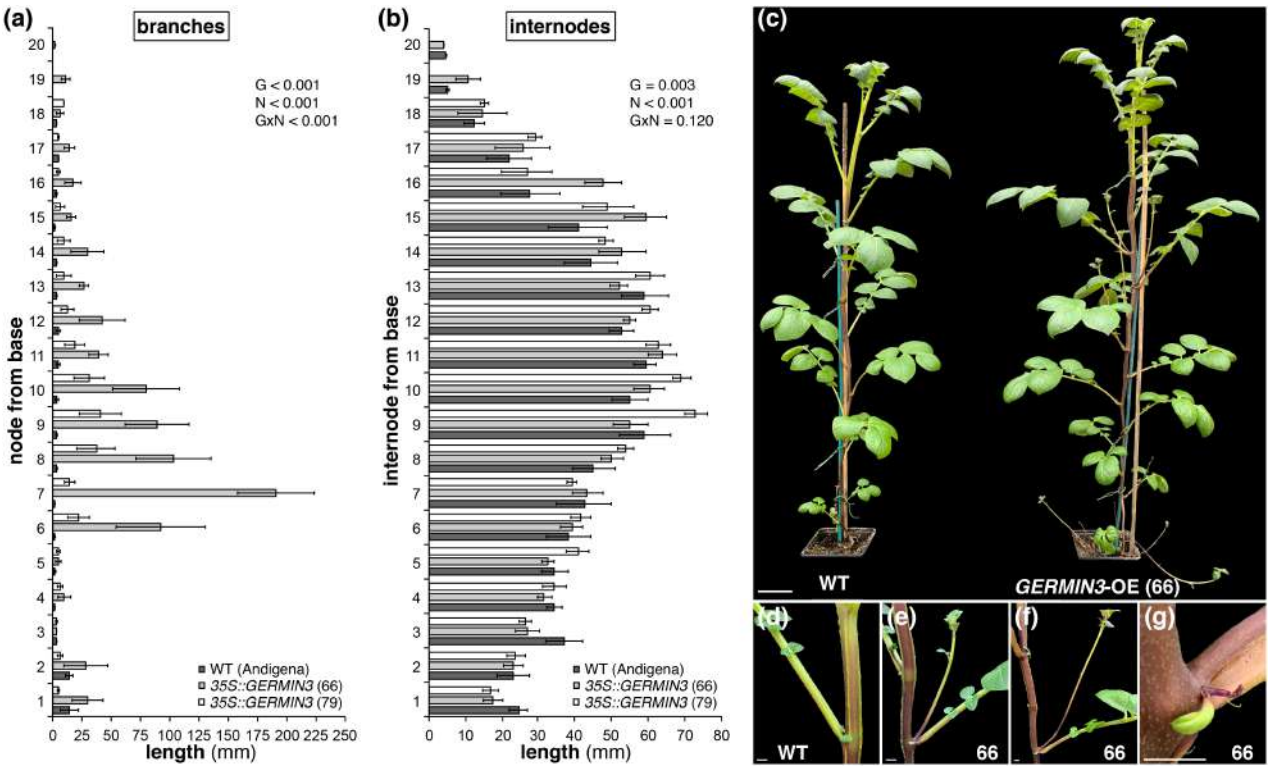

Figure 4. GERMIN3 over-expression results in increased stem axillary bud growth.
GERMIN3 over-expressing lines exhibited stronger axillary bud growth than wild-type *Solanum tuberosum* ssp. *andigena* (a) and have altered stem length at some internodes (b).
These phenotypes caused a more branched appearance and increased plant height (c).
(d–g) Axillary bud and internodal length were measured in six biological replicates 56 days after planting. All data are represented as mean ± SE and the ANOVA *P*-values for the factors genotype (G), node number (N) and their interaction (G × N) are indicated.

determine the upstream determinants of gene expression, we conducted a series of promoter transactivation assays using group A bZIP transcription factors (StbZIP27, StbZIP36, StbZIP35 and StbZIP66) to drive expression of a *GERMIN3::LUC* construct in transient assays. We failed to observe clear activation of expression by any of the bZIPs (data not shown). Unexpectedly, we observed an increase in luminescence in the absence of expression of any exogenous transcription factors after an extended period of measurement that coincided with the end of the putative night (Figure 5d). This increase in luminescence was abolished by inclusion of 2% sucrose in the buffer used to maintain leaf disks, suggesting that *GERMIN3* transcription could be activated by endogenous transcriptional activators in response to starvation.

Transcriptional profiles associated with altered GERMIN3 expression in stolons from transgenic lines

As tuberisation characteristics were altered in the *35S::GERMIN3* lines, we investigated the transcript level for the major tuberisation signal *SP6A* by RT-qPCR in leaves and stolons in WT plants and selected OE lines. *SP6A* was detected in all leaf samples, and no significant differences in abundance were observed between lines (Figure 6a). The *SP6A*-specific transcript was not detected in stolons prior to tuberisation except for line 66; however, transcripts were observed at similar abundances in swelling stolons of both WT and OE lines (Figure 6b). Previously, we have reported that TFL1B is an inhibitor of tuberisation that competes with SP6A for binding to FD and FDL in the tuberigen activation complex (Zhang et al., 2020). In leaves, *TFL1B* transcript abundances were similar in WT and OE lines 66 and 79, although they were more abundant in leaves of *35S::GERMIN3* line 91 (Figure 6c). In hooked stolons, significantly lower levels of *TFL1B* were detected in stolons prior to tuberisation in OE lines than WT controls, although abundance fell in all lines to a similar level following the initiation of stolon swelling (Figure 6d).

Transcriptomic analysis was performed in hooked and swelling stolons of WT and the transgenic *StGERMIN3* OE line 66, selected for its high level of expression and consistent phenotype. Pairwise comparison of hooked and swelling stolons indicated that 5409 transcripts were significantly differentially abundant in WT plants, with 2011 transcripts more abundant and 3398 transcripts less abundant in swelling than hooked stolons. In the GERMIN3 OE line 66, 3722

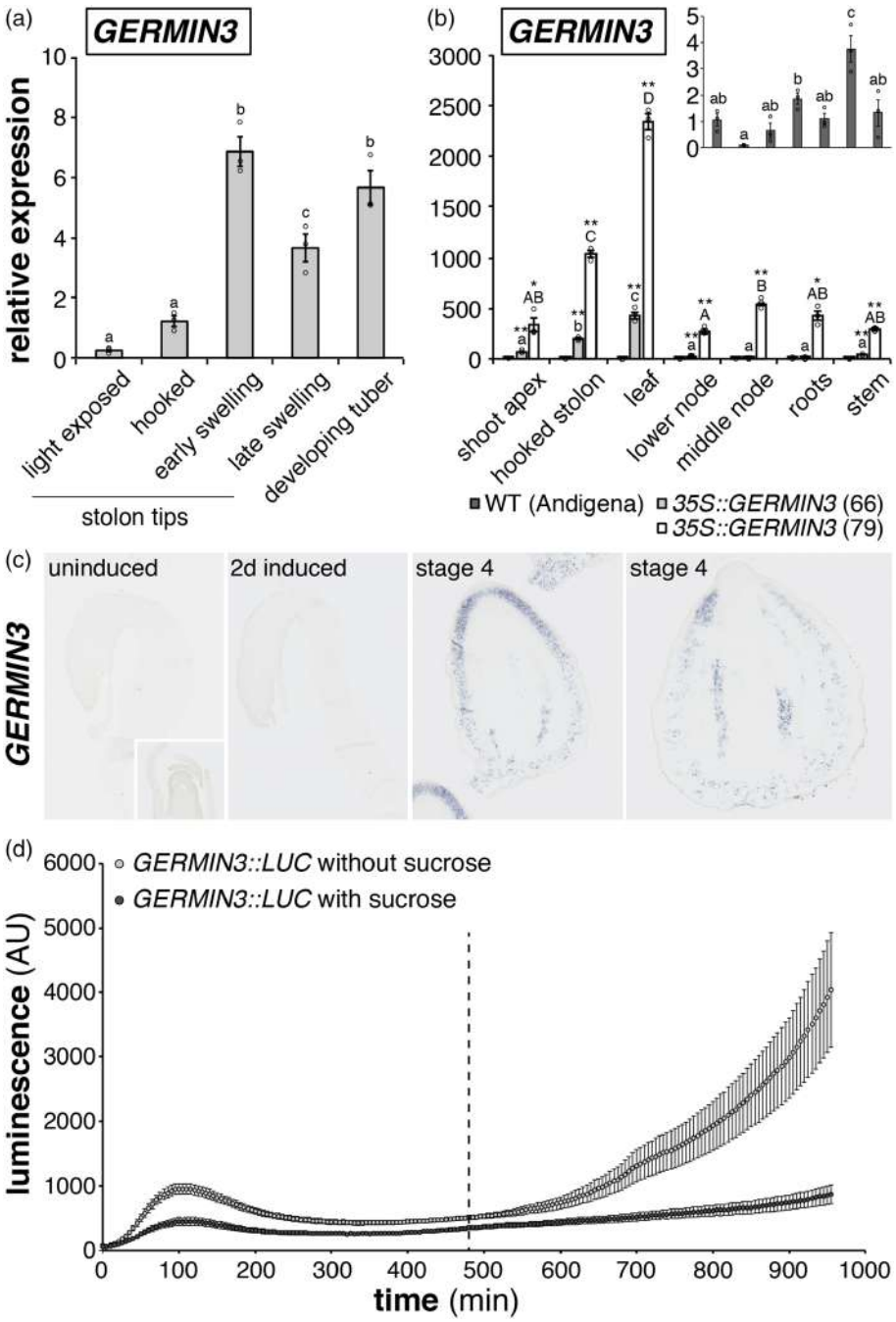

Figure 5. GERMIN3 transcripts are found in multiple organs of *S. tuberosum* ssp. *andigena* and are influenced by developmental and environmental cues.
GERMIN3 transcript abundance quantified in stolon tips and developing tubers of wild-type *Solanum tuberosum* ssp. *andigena* (a), data are presented as mean ± SE (n = 3). Tissues where abundance was significantly different according to Fisher's protected LSD test ($P < 0.05$) are indicated by different letters, and individual data points are shown as circles.
Panel (b) presents a comparison of *GERMIN3* transcript abundance in above and below ground organs of wild type and two over-expressing (OE) lines. Data are presented as mean ± SE (n = 3) with individual data points shown. Letters indicate significant differences in transcript abundance between tissues in each line as determined using Fisher's protected LSD test ($P < 0.05$). Asterisks indicate differences between OE and wild-type lines within a given tissue as determined using the Student's *t*-test.
The inset shows data from wild-type plants on an expanded scale. RNA *in situ* hybridisation was conducted in stolon tips and developing tubers of wild-type *S. tuberosum* ssp. *andigena* using *GERMIN3*-specific antisense probes (c).
The activity of the *GERMIN3* promoter was determined by transient expression of a *GERMIN::LUC* construct in *N. benthamiana* leaves (d). Leaf discs were prepared from the infiltrated leaves at the end of the day and promoter activity measured as luminescence following floating of discs on a buffer in the presence or absence of 2% sucrose. Dotted line indicates the end of the putative night.

transcripts were differentially abundant, with 1451 transcripts more abundant and 2271 less abundant in swelling stolons than in hooked stolons (Table S1). There was significant overlap in the identity of differentially abundant transcripts, with a total of 3233 common transcripts in WT and OE line 66. Of the common transcripts, 1292 were more abundant in swelling stolons of both genotypes, whereas 1941 were less abundant (Figure S5).

This transcriptome analysis demonstrated an extensive level of changes upon tuber initiation in both the WT and *GERMIN3* OE line 66. However, comparison of the two lines at identical stolon developmental stages revealed a relatively small number of differentially expressed genes (DEGs; Figure 6e,f; Table S2). A total of 10 differentially abundant transcripts, all of which were more abundant in the *35S::GERMIN3* line relative to the WT line, were present at the non-initiated hooked stolon stage. In swelling stolons, 50 transcripts exhibited differential abundance, 46 of which were more abundant and 4 less abundant in the *35S::GERMIN3* line relative to the WT line (Figure 6f). All DEG's present in the hooked stage comparison were also present in the swelling stage gene list. A *GERMIN3* gene (Soltu.DM.01G041670) with a nucleotide similarity of 99.8% compared with the DM v4.03 transcript (PGSC0003DMT 400046995) and used in the construction of the over-expressor construct presented in this manuscript was present in both gene lists. A second GLP gene (Soltu.DM.01G041740) was more highly expressed in the swelling stolon stage of the *35S::GERMIN3* line relative to the WT, the product of which may have a similar function to GERMIN3. Many of the remaining transcripts were poorly characterised although the list included cell-wall associated kinases (Soltu.DM.09G009260; Soltu.DM.09G009230 and Soltu.DM.09G009220) with a function in the regulation of cell expansion (Kohorn, 2016) as well as a transcript encoding an ADP-ribosylation factor GTPase (Soltu.DM.01G003520) that plays a role in cell division, expansion and cellulose production (Gebbie et al., 2005). Several transcripts encoding receptor-like kinases and a small number encoding transcription factors were also present within the DEG's list, as were a number of transcripts encoding cytochrome P450s and other oxidoreductases (Table S2).

Analysis of transcripts known to be associated with tuberisation such as *SP6A*, other PEPB's, and a range of transcripts associated with light signalling and circadian regulation indicated similar patterns of expression (Figure S6). Taken together, these data indicate that molecular events associated with tuberisation were largely unaffected by overexpression of the *GERMIN3* gene.

GERMIN3 OE lines exhibit increased oxalate oxidase activity

Many GERMIN and GLP proteins exhibit oxalate oxidase activity (Lane et al., 1993; Sakamoto et al., 2015; Woo et al., 2000). To determine whether GERMIN3 has this activity, oxalate oxidase activity was quantified in extracts from leaves of WT and three highly expressing *35S::GERMIN3* lines. In extracts from WT leaves, 2.89 $\pm$ 0.32 μmol H_2O_2 min^{-1} mg FW^{-1} were generated in the presence of oxalate while the respective values for lines 66, 79 and 91 were 4.78 $\pm$ 0.56, 4.31 $\pm$ 0.52 and 5.49 $\pm$ 0.34 μmol H_2O_2 min^{-1} mg FW^{-1}. Differences between *35S::GERMIN3* and WT lines were all highly significant ($P < 0.01$, 0.05 and 0.001, respectively) according to the Student's *t*-test with increases between 1.5- and 1.9-fold. These data suggest that GERMIN3 protein exhibiting oxalate oxidase activity accumulates in transgenic plants.

GERMIN3 is localised in the endoplasmic reticulum and impacts plasmodesmatal gating

The coding sequences of *GERMIN3* were expressed as C-terminal fusions to red fluorescent protein (RFP). The constructs were introduced to source leaves of *N. benthamiana* expressing an endoplasmic reticulum (ER)-lumen localised GFP (Carette et al., 2000) by biolistic bombardment. Visualisation of the RFP-tagged GERMIN3 was used as a reporter for the presence of GERMIN3, which was localised by confocal microscopy. The protein clearly located to the ER, where it colocalised with the GFP-tagged ER reporter (Figure 7a–c). Counterstaining with aniline blue highlighted the presence of callose associated with plasmodesmata at locations that were frequently localised in close proximity to the ER-localised GERMIN3 (Figure 7d–f).

In order to determine whether GERMIN3 had any impact on plasmodesmal function, we used the plasmodesmatal (PD) gating assay described by Oparka et al. (1999). A plasmid expressing the sporamin-GFP fusion from a 35S promoter was bombarded into source leaves of *N. benthamiana*, and the intercellular movement of the fusion protein was monitored by confocal microscopy. Other leaves were co-bombarded with the GFP:SPORAMIN construct and a construct expressing GERMIN3 tagged with RFP.

In control leaves that were bombarded only with the GFP:SPORAMIN construct, the GFP signal was primarily restricted to the bombarded cell with almost no trafficking to neighbouring cells (Table 1; Figure 8b). This result confirms previous work indicating that the low size exclusion limit of source leaf PD restricts movement of the protein to adjacent cells (Oparka et al., 1999). In contrast, in cells that were co-bombarded and that expressed both the GERMIN3:RFP and GFP:SPORAMIN fusions, the frequency in which the SPORAMIN fusion was observed both in the bombarded cell and in neighbouring cells increased markedly (Table 1) while the GERMIN3 fusion was observed only in the bombarded cell (Figure 8c,d) suggesting that the presence of the GERMIN protein in the bombarded cell

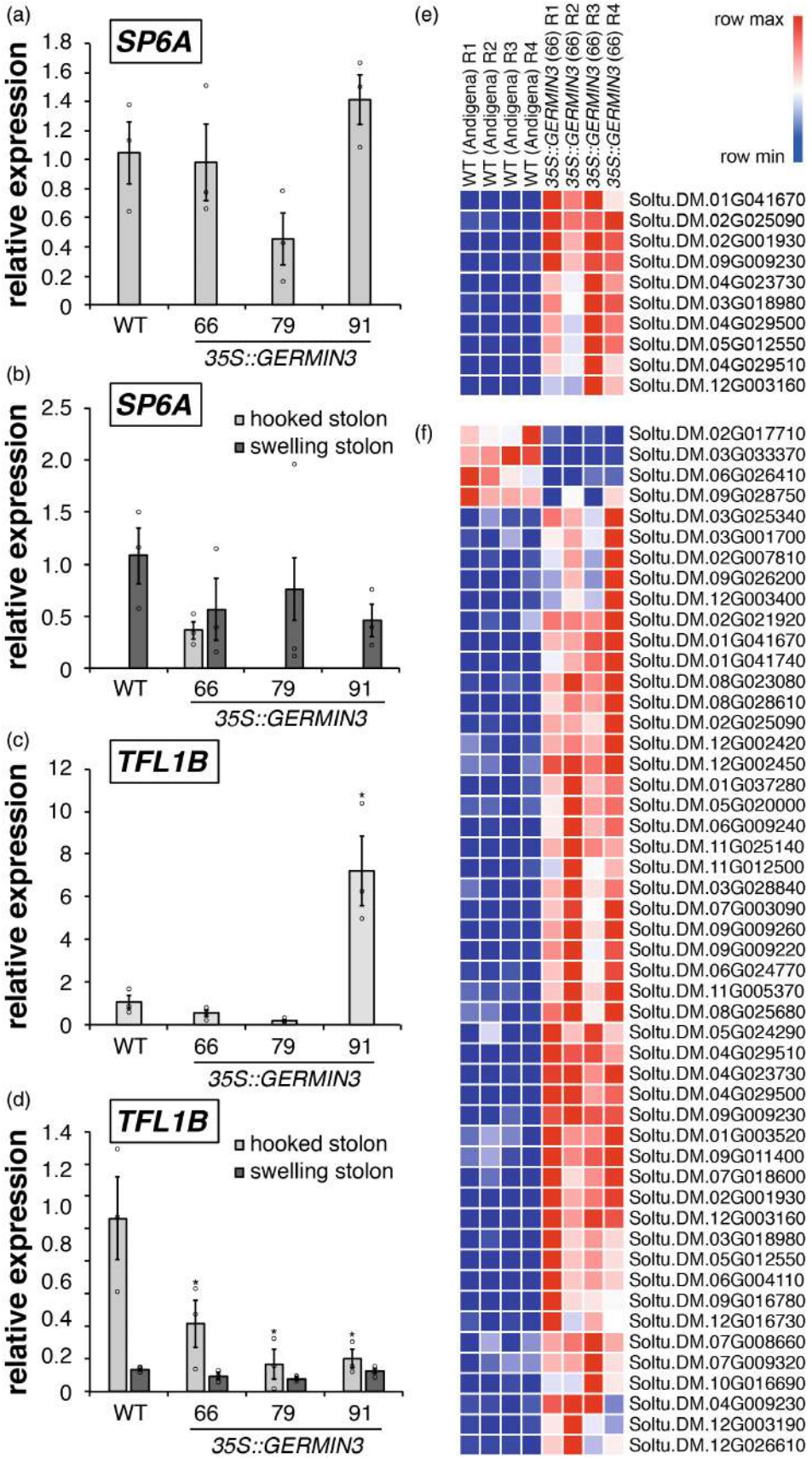

Figure 6. Abundance of key transcripts in stolons of wild-type and GERMIN3 over-expressing (OE) lines.
Abundance of *SP6A* (a, b) and *TFL1B* (c, d) transcripts were quantified by RT-qPCR in leaves (a, c) and stolons (b, d) in ADG *35S::GERMIN3* lines from plants cultivated for 47 days. Expression levels were determined relative to the reference gene *EF1α*. All data are represented as mean values ± SE of three independent biological replicates (with individual data points indicated), and asterisks denote values that were significantly different between transgenic lines and wild-type controls as determined by one-way ANOVA followed by Fisher's protected LSD test ($P < 0.05$).
Transcripts that were significantly differentially abundant between wild-type and OE line 66 are also indicated for hooked (e) and swelling (f) stolons, with each row showing relative abundance in individual replicates. Transcript identity is indicated to the right of each row, and further details are provided in Table S2.

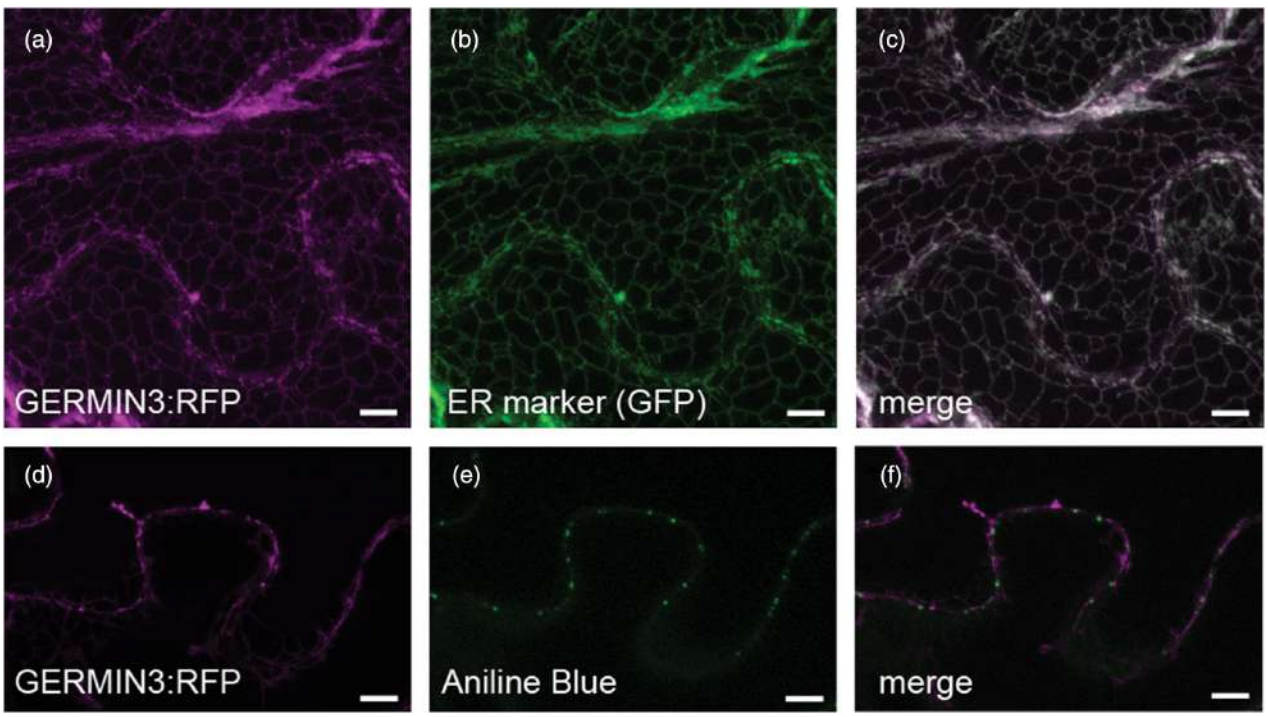

Figure 7. Intracellular localisation of GERMIN3:RFP.
The GERMIN3:RFP fusion protein (a) localised to the endoplasmic reticulum as indicated by co-localisation with the GFP:ERD2 marker (b, c).
A single stack of GERMIN3:RFP (d) indicates a close association with callose deposits at the neck of plasmodesmata stained with aniline blue (e, overlay in f).
Scale bars represent 10 μm.

increased the size exclusion limit of PD, allowing passage of the GFP:SPORAMIN fusion between cells. The fact that the GERMIN3:RFP was retained only in the bombarded cell despite having a similar molecular weight to GFP:SPORAMIN suggests that different mechanisms exist for regulating protein trafficking via the lumen of the desmotubule compared with trafficking via the cytoplasmic space between the cell wall and the desmotubule within the PD pore.

The results from the PD gating assays provide evidence for the function of GERMIN3. However, it is unknown whether the oxalate oxidase activity of the protein is necessary for its gating effect. The structure of many GERMIN and GLPs has been determined (e.g. da Cruz et al., 2019). The enzyme is a metalloprotein and binding of an Mn atom is required not only for oxalate oxidase but also for reported superoxide dismutase activity (Woo et al., 2000). The amino acid residues involved in Mn binding have been clearly identified (da Cruz et al., 2019; Sakamoto et al., 2015), and sequence alignment with potato GERMIN3 enables the corresponding residues (three histidine and a glutamic acid residue) to be identified in this protein. We synthesised a mutated GERMIN3 in which the Mn-binding residues were changed (Figure 8a). We then used this mutated form in the gating assays where we found that the mutant protein exhibited a similar capacity to induce PD gating as the native protein (Table 1; Figure 8e,f). These data indicate that Mn-binding and oxalate oxidase/superoxide dismutase activities are not required for PD gating.

DISCUSSION

Regulation of the tuber life cycle

Tuber life cycle processes in potato are heavily regulated, enabling the interface with environmental signalling to

Table 1 SPORAMIN:GFP movement in *Nicotiana benthamiana* epidermal cells

	Construct					
	GFP: SPORAMIN		GFP: SPORAMIN		GFP: SPORAMIN	
	-		GERMIN3:RFP		mGERMIN3: RFP	
Experiment	Single cell	>1 cell	Single cell	>1 cell	Single cell	>1 cell
1	13	1	2	27		
2	90	2	33	12		
3			88	46		
4			1	17	4	18

Nicotiana benthamiana leaves were bombarded with particles coated with constructs for the expression of GFP:SPORAMIN alone, GFP:SPORAMIN and GERMIN3:RFP or GFP:SPORAMIN and mGERMIN3:RFP carrying mutations in the Mn-binding site required for enzyme activity. Leaves were observed under a Zeiss LSM710 upright confocal laser scanning microscope (CLSM; Zeiss, Jena, Germany) Using excitation wavelengths of 488 and 561 for GFP and RFP, respectively, with corresponding emission collected at 500–530 for GFP and 590–630 nm for RFP. The table indicates the number of observations in which GFP fluorescence was restricted to a single cell or in which fluorescence was observed in more than one cell.

optimise and balance vegetative and reproductive growth and development. Significant progress has been made in recent years in our understanding of tuberisation signalling, leading to a detailed model for tuberisation control (Kondhare et al., 2020; Zierer et al., 2021). As well as the FT orthologue, SP6A, other phloem mobile elements are important in tuberisation signalling (Hannapel et al., 2017). These include *BEL5* mRNA, the transcripts for other *BEL* family members (Ghate et al., 2017) and a number of small regulatory RNAs that impact tuberisation signalling (Eviatar-Ribak et al., 2013; Lehretz et al., 2019; Martin et al., 2009).

These tuberisation signalling mechanisms converge on the tuberigen activation complex (TAC) that transcriptionally controls the cascade of gene expression that results in tuber formation. Our prior research identified *GERMIN3* as a target of TAC regulation, and here we aimed to understand its detailed role in the tuber life cycle and plant architecture.

Over-expression of GERMIN3 accelerates meristem activation

The impact of constitutive *GERMIN3* expression on tuber development clearly demonstrated a positive effect on tuber yield, corresponding to the expression level in multiple independent transgenic lines. This was the case for batches of plants harvested 47 and 93 days after planting. These experiments were conducted in plants grown in pots and so may not reflect yields in the field; nevertheless, there is clear potential for *GERMIN3* over-expression to have a positive impact under field conditions. In particular, the observation that *GERMIN3* acts downstream of the TAC provides an opportunity to maintain yields under conditions that impair TAC activation, such as elevated temperature (Koch et al., 2024). Such an approach may be particularly beneficial if combined with transgenic manipulation of potato sink–source relationships using previously identified routes (Lehretz et al., 2021).

Over-expression of *GERMIN3* also resulted in other phenotypes associated with meristem activation processes. There was a significant effect on tuber sprouting, with enhanced bud activity in the OE lines resulting in the growth of more stems per tuber. Above-ground plant architecture was also impacted in *35S::GERMIN3* lines, with a significantly higher stem-branched structure caused by the activation of axillary buds.

GERMIN3 controls PD gating, supporting previous models of tuberisation/dormancy release

The study of Ham et al. (2012) provided evidence that several GLPs are located in the PD where they have a role in the control of cell-to-cell trafficking. However, we are unaware of further work that extends these results. In this study, the GERMIN3:RFP fusion protein was clearly localised to the ER. The ER is an essential component of PD, the membrane-lined pores that interconnect plant cells. The desmotubule which traverses the centre of a plasmodesma is formed from, and continuous with, the cortical ER (Wright & Oparka, 2006) and so our localisation studies are consistent with a PD function.

Previously, we have shown that PD gating plays a significant role in the regulation of the potato tuber life cycle. Our initial studies demonstrated that the early stages of tuber initiation were associated with a switch from apoplastic to symplastic phloem unloading (Viola et al., 2001) allowing a more efficient flux of photoassimilates from source tissues to the developing tubers. This was later further reinforced by the finding that the mobile tuberisation signal SP6A binds to the SWEET11 efflux transporter, preventing efflux from the phloem and redirecting sugar flux to the developing tuber (Abelanda et al., 2019). We also demonstrated that PD gating plays a role in the tuber bud dormancy, where we observed that dormant buds were symplastically isolated and that symplastic reconnection coincided with the first visible signs of dormancy release (Viola et al., 2007). Hence, the regulation of PD gating impacts meristem activation, influencing multiple processes in the potato tuber life cycle (Hancock et al., 2008).

These previous observations suggest a potential mechanism by which GERMIN3 could influence tuberisation; we therefore wished to investigate whether GERMIN3 impacted on PD gating as observed in Arabidopsis. Using

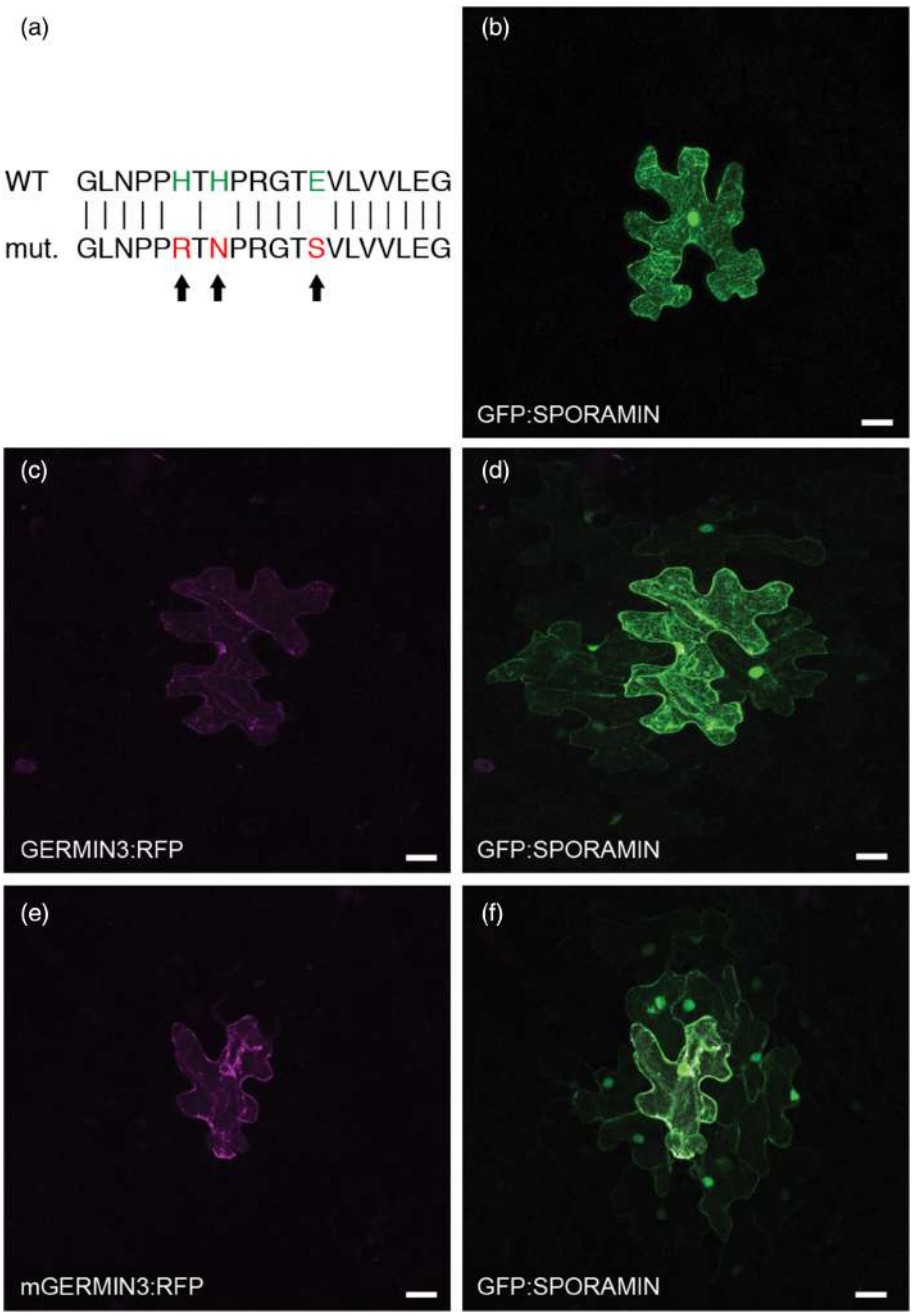

Figure 8. Plasmodesmal gating activity of wild-type and mutant Germin-RFP.
Nicotiana benthamiana leaves were bombarded with plasmids encoding GFP:SPORAMIN alone (b) or co-bombarded with wild-type GERMIN3:RFP and GFP:SPORAMIN (c, d).
Alternatively, leaves were co-bombarded with a mutated GERMIN3:RFP (e) in which the Mn-binding residues were changed to abolish binding (a) and the GFP:SPORAMIN construct (f). Scale bars represent 20 μm.

a well-established cell-to-cell trafficking assay, we clearly demonstrated the impact of GERMIN3 expression, results that strongly suggest a role in the control of PD gating.

Most GLP research implies the impact of these enzymes is due to their oxalate oxidase or superoxide dismutase activities, which are dependent on the amino acid ligands required for Mn binding (Woo et al., 2000). We generated GERMIN3 mutated in these ligands to abolish Mn binding and oxalate oxidase activity. The mutated form of the GERMIN3 retained activity in the cell-to-cell trafficking assay comparable to that of the WT GERMIN3. These data demonstrate that the oxalate oxidase activity of GERMIN3 is not

required for the trafficking function. Further mutation studies will be required to identify the GERMIN features that give rise to enhanced cell-to-cell trafficking. The experimental approach used in this study provides a tractable system for unravelling these effects. Moreover, given that GERMIN3 is present throughout the ER and not only at PD, it is likely that the interaction of GLP with other proteins is required to activate their gating function. Detailed protein–protein interaction studies will shed further light on the precise mechanism of GERMIN3 activity.

Concluding remarks

We propose that GERMIN3 and potentially other GERMIN proteins may have a role in the control of PD gating, activating the switch from apoplastic to symplastic phloem unloading, marking the process of tuber initiation and impacting tuber sprouting in storage and above-ground stem branching. GERMIN3 acts downstream of the tuberigen activation complex and hence regulates tuberisation independently of environmental control. GERMIN3 is therefore a strong candidate for breeding and biotechnology for improved tuber yield in a wide variety of environments.

MATERIALS AND METHODS

Plant material and growth conditions

Solanum tuberosum ssp. *andigena* accession 7540 (ADG) WT plants used for transformation were propagated in 90 mm Petri dishes containing MS medium (Murashige & Skoog, 1962) supplemented with 20 g L^{-1} sucrose and 8 g L^{-1} agar at 18 ± 4°C, 16 h light, light intensity 100 μmol m^{-2} sec^{-1}. Four-week-old *in vitro* sub-cultured plantlets were transferred to 12 cm pots containing compost and grown in a glasshouse under conditions of 16 h light (18°C) and 8 h dark (15°C). Light intensity ranged from 400 to 1000 μmol m^{-2} sec^{-1}. After 6 weeks, plants were moved to a controlled environment growth room under conditions of 10 h light (18°C, 80% humidity) and 14 h dark (15°C, 70% humidity), light intensity 300 μmol m^{-2} sec^{-1} and watered daily.

Generation of GERMIN3 transgenic potato lines

The binary construct used in this study was built based on the GoldenBraid system (gb.cloning.org) (Sarrion-Perdigones et al., 2011). Gene-specific primers containing flanking *Bsm*B1 sites were used to amplify the full-length *GERMIN3* coding sequence (PGSC0003DMT400046995). The PCR-purified fragments were ligated into a pUPD entry vector using the *Bsm*BI digestion–ligation reaction protocol and confirmed by Sanger sequencing. Assembly reactions with the p2x35S (GB0222) promoter and pTnos terminator (GB0037) using *Bsa*I and *Bsm*BI (New England Biolabs, Ipswich, MA, USA) as restriction enzymes in 25-cycle digestion/ligation reactions were performed essentially as described by Sarrion-Perdigones et al. (2011). The resulting pDGB1_alpha1:p2x35S:StGERMIN:pTnos transcriptional unit was further combined with the pDGB2:pPnos:NptII:Tnos transcriptional unit in pDGB1_omega2 to form the final construct. Final binary vectors were transformed into *Agrobacterium tumefaciens* strain LBA4404. *Agrobacterium*-mediated potato transformation was performed as described previously (Ducreux et al., 2005).

Promoter transactivation assays

A 3 kb DNA fragment immediately upstream of the start ATG codon of *GERMIN3* was fused to the firefly luciferase (*LUC*) reporter gene and cloned into a pGWB vector backbone. The resulting vector was transformed into *Agrobacterium* strain GV3101. The CDS of group A bZIPs 2, 27 (FDL1a), 36, 35 and 66 were PCR amplified from cDNA obtained from *S. tuberosum* ssp. *andigena* and cloned after the *UBI10* promoter to provide constitutive expression. The respective vectors were transformed into *Agrobacterium* strain GV3101.

Agrobacteria carrying the respective plasmids were grown overnight and diluted to achieve an OD600 nm of 0.1. The cultures were incubated until they reached an OD600 nm of 1.0. Cells were pelleted by centrifugation (3000 ***g***, 22°C, 17 min) and resuspended in a 5% (w/v) sucrose solution to achieve a final OD600 nm of 0.2. For the transactivation assays, cultures of the *GERMIN3::LUC-containing* Agrobacteria and the respective bZIPs were mixed in a ratio of 1:1 and brought to a final OD600 nm of 0.2. For the promoter-only control, an *Agrobacterium* strain without a transferable plasmid was used for mixing with the reporter construct-carrying strain. The resulting agrobacteria suspensions were infiltrated into leaves of three different plants from 5-week-old *N. benthamiana* plants. Each construct or combination of constructs was infiltrated into individual leaves to avoid cross-contamination.

Two days after infiltration, a total of 12 leaf discs from three different plants from three different leaves were prepared using a 5 mm cork borer and floated on top of 100 μl of incubation solution (½ MS salts; 5 mM MES pH 6.0) in wells of a white, flat-bottom, chimney, 96-well plate. Samples were incubated for 30 min at 22°C in the light. Then, 100 μl of assay solution (½ MS salts; 5 mM MES pH 6.0; 40 μM D-luciferin) was added to each sample. The plate was immediately subjected to luminescence measurement in a TECAN Spark plate reader. Light was detected between 500 and 750 nm, signal integration time was set to 2 sec per sample per measurement, measurement interval was 5 min, and samples were kept in complete darkness at 25°C during the whole measurement period of 16 h.

In order to perform the extended night treatment, leaf discs were harvested right before the start of the regular night in the greenhouse, where the *N. benthamiana* plants were grown in a 16 h light/8 h dark cycle at 25°C. The 480-min measuring time point marks the onset of the extended night treatment. For the samples containing 2% (w/v) sucrose, the assay solution was supplemented with 2% (w/v) sucrose.

RNA extraction and qRT-PCR

Total RNA was extracted from various potato plant tissues using a RNeasy® Plant Mini Kit (Qiagen, https://www.qiagen.com/), following the manufacturer's instructions. The first-strand cDNA templates were generated by reverse transcription using a double-primed RNA to cDNA EcoDry™ Premix kit (TaKaRa, Clontech, https://www.takarabio.com/about/our-brands/clontech). Potato elongation factor 1-alpha (EF1-α) primers were used as a normalisation control (Nicot et al., 2005). The expression levels of StGERMIN, StCEN/TFL1B and StSP6A were determined using the StepOnePlus real-time PCR system (Applied Biosystems, https://www.thermofisher.com/uk/en/home/brands/applied-biosystems.html) and StepOne Software version 2.3 (Applied Biosystems). Gene-specific primers and Universal Probe Library (UPL; Roche Life Science, https://lifescience.roche.com/) probes (Table S3) were used at a concentration of 0.2 and 0.1 μM, respectively.

Thermal cycling conditions were 10 min denaturation at 95°C followed by 40 cycles of 15 sec at 94°C and 60 sec at 60°C. Relative expression levels were calculated and the primers validated using the Delta–Delta Ct method (Livak & Schmittgen, 2001).

RNA *in situ* hybridisation

RNA *in situ* hybridisation was performed as described by Gramma and Wahl (2023). Briefly, tissue samples were taken at the end of the day and were immediately transferred into freshly prepared FAA fixative (formaldehyde–acetic acid–ethanol). Samples were subsequently dehydrated with ethanol and infiltrated with paraffin wax (Paraplast; Leica Microsystems (UK) Ltd, Sheffield, UK) using an automated vacuum-embedding system (ASP300S, Leica Microsystems). After infiltration, samples were processed in an embedding centre (EG1160, Leica Microsystems). Using a rotary microtome (RM2265; Leica Microsystems), 8 μm sections were made and transferred to polysine-coated slides (VWR, Lutterworth, UK). A full-length *GERMIN3* probe (PGSC0003DMT400046995) was amplified from cDNA, cloned into the pGEM®-T Easy Vector (Promega UK Ltd, Southampton, UK) and synthesised with a Roche DIG RNA labelling kit (Merck Life Science UK Limited, Gillingham, UK). Sections were scanned by the Axio Scan.Z1 slide scanner (Zeiss, Jena, Germany).

RNA-seq and transcriptomics analysis

Total RNA was quality checked using a Bioanalyzer 2100 (Agilent, Stockport, UK) and sequencing libraries constructed using a Stranded mRNA Prep kit (Illumina, Cambridge, UK), each from 500 ng RNA, as recommended. QC of libraries was performed using a Bioanalyzer 2100 and, following equimolar pooling of all 16 samples, RNA-seq was carried out on a NextSeq 2000 (Illumina) sequencer loaded at 750 pM. Fastq data were demultiplexed on completion, prior to downstream analysis.

The RNA-seq reads were pre-processed to remove adapters using Fastp (Chen et al., 2018). Low-quality reads, defined by a length <30 or a quality score <20, were eliminated. The processed reads were mapped to a high-quality potato reference transcriptome, which was assembled from a combination of RNA-seq short-reads and Iso-seq long-reads in a DM potato study (unpublished), using Salmon (Patro et al., 2017). The 3D RNA-seq App was applied to study the gene and transcript expression changes between WT and line 66 (L66) as well as samples exhibiting swelling and hooked phenotypes (Guo et al., 2021). Genes and transcripts with significant expression changes were determined with adjusted *P*-value <0.05 and absolute $\log_2$-fold-change ≥1.

Oxalate oxidase assay

Total oxalate oxidase activity was evaluated using an oxalate assay kit (Abcam Limited, Cambridge, UK; ab241007) to quantify H_2O_2 production in the presence of oxalate following the manufacturer's protocol. A total of 20 mg of fresh frozen leaf tissue was ground and resuspended in 200 μl ice-cold oxalate oxidase assay buffer, then incubated for 10 min on ice. Following incubation, samples were centrifuged for 20 min at 10 000 ***g*** and 100 μl of the supernatant collected. Proteins were precipitated by addition of 200 μl 4.32 M ammonium sulphate, followed by a 30 min incubation on ice. Precipitated proteins were collected by centrifugation (10 000 ***g***, 30 min), the supernatant discarded, and protein resuspended in 100 μl fresh buffer to remove metabolites that may interfere with the assay. Forty microlitres of the reconstituted sample was then used in the final quantification assay.

Construction of GERMIN-mRFP

The *GERMIN3* sequence was amplified from a template encoding GERMIN3 DMT46995-B3-B5 (Thermofisher Scientific, https://www.thermofisher.com/uk/en/home.html) using attB adapter-flanked primers (GERMIN-FOR; 5′-AAAAAAGCAGGCTTCGAAGGAGATAGAACCATGGCTCTCAAGTACTTTGTATTAAC-3′ and GERMIN-REV; 5′-GGGGACCACTTTGTACAAGAAAGCTGGGTGGTTGTTATCCCACCAGAATTG-3′). The amplicon was recombined into pDONR207 using Gateway BP Clonase II (Thermofisher Scientific), then recombined into plasmid pK7RWG2 (Karimi et al., 2007) using Gateway LR Clonase II (Thermofisher Scientific).

Live-cell imaging of Germin-mRFP

Agrobacterium tumefaciens cultures (strain AGL1) carrying the GERMIN3:RFP plasmid construct were prepared at OD600 nm = 0.1 and infiltrated into the lower surface of *N. benthamiana* leaves expressing the ER marker GFP-ERD2 (Carette et al., 2000). For callose staining, sample leaves were infiltrated with aniline blue stain 0.05% in 0.067 M phosphate buffer, pH 8.5. Imaging of GERMIN3:RFP was performed on a Zeiss LSM 710 upright confocal laser scanning microscope (CLSM; Zeiss) using a 40× objective, with an RFP excitation wavelength of 561 nm and emission collected at 590–630 nm. For aniline blue imaging, an excitation wavelength of 405 nm was used and emission collected at 420–480 nm.

Gating experiment

N. benthamiana leaf epidermal cells were co-bombarded with mixtures of plasmid DNA by particle bombardment using a Handgun essentially as described by Gal-On et al. (1997). The plasmid mixtures comprised *35S::GFP:SPORAMIN* (Oparka et al., 1999) and *pK7RWG2::GERMIN3* (GERMIN3:RFP). Co-bombarded cells were examined by CLSM 2 days after bombardment. Cells were imaged using a 20× objective with both GFP and RFP imaged sequentially: GFP excitation at 488 nm, emission at 500–530 nm, RFP excitation at 561 nm and emission at 590–630 nm.

AUTHOR CONTRIBUTIONS

RC: Investigation, writing – original draft; GC: Investigation; BW: Investigation, writing – original draft; LJMD: Investigation, resources; JD: Investigation, resources; WG: Formal analysis; RZ: Formal analysis; JAM: Investigation; PH: Data curation; VW: Investigation, Resources, Supervision, writing – original draft, writing – review and editing; MAT: Conceptualisation, Writing – original draft, Supervision, Project administration, Funding acquisition; RDH: Conceptualisation, Writing – original draft, Writing – review and editing, Supervision, Project administration, Funding acquisition.

ACKNOWLEDGEMENTS

This work was funded by the EU Horizon 2020 research and innovation programme ADAPT (Accelerated Development of Multiple Stress Tolerant Potato) grant agreement number GA 2020 862-858 and the Scottish Government Rural and Environmental Science and Analytical Services Division as part of the strategic research programme 2022–2027.

CONFLICT OF INTEREST

The authors declare no conflicts of interest.

DATA AVAILABILITY STATEMENT

The data that support the findings of this study are available in the supplementary material of this article.

SUPPORTING INFORMATION

Additional Supporting Information may be found in the online version of this article.

Figure S1. Tuberisation phenotype of *Solanum tuberosum* ssp. *andigena* wild-type (a) and 35S::GERMIN3 line 66 (b).

Figure S2. Impact of altered expression of GERMIN3 on tuber yield in *Solanum tuberosum* cv. Desiree.

Figure S3. Impact of altered expression of GERMIN3 on aerial phenotype of *Solanum tuberosum* cv. Desiree.

Figure S4. Flowering phenotype of *Solanum tuberosum* ssp. *andigena* wild-type and GERMIN3 over-expressing line.

Figure S5. Common and unique differentially abundant transcripts in hooked and swelling stolons of wild-type and GERMIN3 over-expressing *Solanum tuberosum* ssp. *andigena* potato genotypes.

Figure S6. Relative abundance of transcripts associated with tuberisation, light signalling, and circadian regulation in stolons of wild-type and GERMIN3 over-expressing *Solanum tuberosum* ssp. *andigena* potato genotypes.

Table S1. Relative abundance of transcripts in swelling compared with hooked stolons in *Solanum tuberosum* subsp. *andigena*.

Table S2. Transcripts exhibiting significant differences in stolons between wild-type and GERMIN3 over-expressing line 66 genotypes.

Table S3. Primers and probes used for RT-qPCR.

REFERENCES

Abe, M., **Kobayashi, Y.**, **Yamamoto, S.**, **Daimon, Y.**, **Yamaguchi, A.**, **Ikeda, Y.** ***et al.*** (2005) FD, a bZIP protein mediating signals from the floral pathway integrator FT at the shoot apex. *Science*, **309**, 1052–1056. Available from: https://doi.org/10.1126/science.1115983

Abelanda, J.A., **Bergonzi, S.**, **Oortwijn, M.**, **Sonnewald, S.**, **Du, M.**, **Visser, R.G.F.** ***et al.*** (2019) Source-sink regulation is mediated by interaction of an FT homolog with a SWEET protein in potato. *Current Biology*, **29**, 1178–1186. Available from: https://doi.org/10.1016/j.cub.2019.02.018

Berna, A. & **Bernier, F.** (1999) Regulation by biotic and abiotic stress of a wheat germin gene encoding oxalate oxidase, a H_2O_2-producing enzyme. *Plant Molecular Biology*, **39**, 539–549. Available from: https://doi.org/10.1023/a:1006123432157

Carette J.E., **Stuiver M.**, **van Lent J.**, **Wellink J.** & **van Kammen A.** (2000) Cowpea mosaic virus infection induces a massive proliferation of endoplasmic reticulum but not golgi membranes and is dependent on de novo membrane synthesis. *Journal of Virology*, **74**, 6556–6563. Available from: https://doi.org/10.1128/jvi.74.14.6556-6563.2000.

Chen, S., **Zhou, Y.**, **Chen, Y.** & **Gu, J.** (2018) fastp: an ultra-fast all-in-one FASTQ preprocessor. *Bioinformatics*, **34**(17), i884–i890. Available from: https://doi.org/10.1093/bioinformatics/bty560

da Cruz, W.T., **Bezerra, E.H.S.**, **Grangeiro, T.B.**, **Lopes, J.L.S.**, **Silva, M.Z.R.**, **Ramos, M.V.** ***et al.*** (2019) Structural and enzymatic characterization of peruvianin-I, the first germin-like protein with proteolytic activity. *International Journal of Biological Macromolecules*, **126**, 1167–1176. Available from: https://doi.org/10.1016/j.ijbiomac.2019.01.023

Davidosn, R.M., **Reeves, P.A.**, **Manosalva, P.M.** & **Leach, J.E.** (2009) Germins: a diverse protein family important for crop improvement. *Plant Science*, **177**(6), 499–510. Available from: https://doi.org/10.1016/j.plantsci.2009.08.012

Ducreux, L.J.M., **Morris, W.L.**, **Hedley, P.E.**, **Shepherd, T.**, **Davis, H.V.**, **Millam, S.** ***et al.*** (2005) Metabolic engineering of high carotenoid potato tubers containing enhanced levels of β-carotene and lutein. *Journal of Experimental Botany*, **56**(409), 81–89. Available from: https://doi.org/10.1093/jxb/eri016

Dunwell, J.M., **Gibbings, J.G.**, **Mahmood, T.** & **Saqlan Naqvi, S.M.** (2008) Germin and germin-like proteins: evolution, structure, and function. *Critical Reviews in Plant Sciences*, **27**(5), 342–375. Available from: https://doi.org/10.1080/07352680802333938

Eviatar-Ribak, T., **Shalit-Kaneh, A.**, **Chappell-Maor, L.**, **Amsellem, Z.**, **Eshed, Y.** & **Lifschitz, E.** (2013) A cytokinin-activating enzyme promotes tuber formation in tomato. *Current Biology*, **23**(12), 1057–1064. Available from: https://doi.org/10.1016/j.cub.2013.04.061

Gal-On, A., **Meiri, E.**, **Elman, C.**, **Gray, D.J.** & **Gaba, V.** (1997) Simple hand-held devices for the efficient infection of plants with viral-encoding constructs by particle bombardment. *Journal of Virological Methods*, **64**(1), 103–110. Available from: https://doi.org/10.1016/S0166-0934(96)02146-5

Gangadhar, B.H., **Mishra, R.K.**, **Kappachery, S.**, **Baskar, V.**, **Venkatesh, J.**, **Nookaraju, A.** ***et al.*** (2021) Enhanced thermo-tolerance in transgenic potato (*Solanum tuberosum* L.) overexpressing hydrogen peroxide-producing germin-like protein (GLP). *Genomics*, **113**(5), 3224–3234. Available from: https://doi.org/10.1016/j.ygeno.2021.07.013

Gebbie, L.K., **Burn, J.E.**, **Hocart, C.H.** & **Williamson, R.E.** (2005) Genes encoding ADP-ribosylation factors in *Arabidopsis thaliana* L. Heyn.; genome analysis and antisense suppression. *Journal of Experimental Botany*, **56**(414), 1079–1091. Available from: https://doi.org/10.1093/jxb/eri099

Ghate, T.H., **Sharma, P.**, **Kindhare, K.R.**, **Hannapel, D.J.** & **Banerjee, A.K.** (2017) The mobile RNAs, StBEL11 and StBEL29, suppress growth of tubers in potato. *Plant Molecular Biology*, **93**(6), 563–578. Available from: https://doi.org/10.1007/s11103-016-0582-4

Gramma, V. & **Wahl, V.** (2023) RNA in situ hybridization on plant tissue sections: expression analysis at cellular resolution. *Methods in Molecular Biology*, **2686**, 331–350. Available from: https://doi.org/10.1007/978-1-0716-3299-4_17

Guo, W., **Tzioutziou, N.A.**, **Stephen, G.**, **Milne, I.**, **Calixto, C.P.G.**, **Waugh, R.** ***et al.*** (2021) 3D RNA-seq: a powerful and flexible tool for rapid and accurate differential expression and alternative splicing analysis of RNA-seq data for biologists. *RNA Biology*, **18**(11), 1574–1587. Available from: https://doi.org/10.1080/15476286.2020.1858253

Ham, B.K., **Li, G.**, **Kang, B.H.**, **Zeng, F.** & **Lucas, W.J.** (2012) Overexpression of Arabidopsis plasmodesmata germin-like proteins disrupts root growth and development. *Plant Cell*, **24**(9), 3630–3648. Available from: https://doi.org/10.1105/tpc.112.101063

Han, X., **Huang, L.J.**, **Feng, D.**, **Jiang, W.**, **Miu, W.** & **Li, N.** (2019) Plasmodesmata-related structural and functional proteins: the long sought-after secrets of a cytoplasmic channel in plant cell walls. *International Journal of Molecular Sciences*, **20**(12), 2946. Available from: https://doi.org/10.3390/ijms20122946

Hancock, R.D., **Morris, W.L.**, **Ducreux, L.J.M.**, **Morris, J.A.**, **Usman, M.**, **Verrall, S.R.** ***et al.*** (2014) Physiological, biochemical and molecular responses of the potato (*Solanum tuberosum* L.) plant to moderately elevated temperature. *Plant, Cell & Environment*, **37**(2), 439–450. Available from: https://doi.org/10.1111/pce.12168

Hancock, R.D., **Roberts, A.G.** & **Viola, R.** (2008) A role for symplastic gating in the control of the potato tuber life cycle. *Plant Signaling & Behavior*, **3**, 27–29. Available from: https://doi.org/10.4161/psb.3.1.4813

Hannapel, D.J., **Sharma, P.**, **Lin, T.** & **Banerjee, A.K.** (2017) The multiple signals that control tuber formation. *Plant Physiology*, **174**(2), 845–856. Available from: https://doi.org/10.1104/pp.17.00272

Ilyas, M., **Irfan, M.**, **Mahmood, T.**, **Hussain, H.** & **Naeem, I.** (2020) Analysis of germin-like protein genes (OsGLPs) family in rice using various in silico approaches. *Current Bioinformatics*, **14**(1), 17–33. Available from: https://doi.org/10.2174/1574893614666190722165130

Jackson, S.D., **Heyer, A.**, **Dietze, J.** & **Prat, S.** (1996) Phytochrome B mediates the photoperiodic control of tuber formation in potato. *The Plant Journal*, **9**(2), 159–166. Available from: https://doi.org/10.1046/j.1365-313X.1996.09020159.x

Karimi, M., **Bleys, A.**, **Vanderhaeghen, R.** & **Hilson, P.** (2007) Building blocks for plant gene assembly. *Plant Physiology*, **145**(4), 1183–1191. Available from: https://doi.org/10.1104/pp.107.110411

Koch, L., **Lehretz, G.G.**, **Sonnewald, U.** & **Sonnewald, S.** (2024) Yield reduction caused by elevated temperatures and high nitrogen fertilization is mitigated by SP6A overexpression in potato (*Solanum tuberosum* L.).

The Plant Journal, **117**(6), 1702–1715. Available from: https://doi.org/10.1111/tpj.16679

Kohorn, B.D. (2016) Cell wall-associated kinases and pectin perception. *Journal of Experimental Botany*, **67**(2), 489–494. Available from: https://doi.org/10.1093/jxb/erv467

Kondhare, K.R., **Natarajan, B.** & **Banerjee, A.K.** (2020) Molecular signals that govern tuber development in potato. *International Journal of Developmental Biology*, **64**, 133–140. Available from: https://doi.org/10.1387/ijdb.190132ab

Lane, B.G., **Dunwell, J.M.**, **Ray, J.A.**, **Schmitt, M.R.** & **Cuming, A.C.** (1993) Germin, a protein marker of early plant development, is an oxalate oxidase. *The Journal of Biological Chemistry*, **268**(17), 12239–12242.

Lehretz, G.G., **Sonnewald, S.**, **Hornyik, C.**, **Corral, J.M.** & **Sonnewald, U.** (2019) Post-transcriptional regulation of FLOWERING LOCUS T modulates heat-dependent source-sink development in potato. *Current Biology*, **29**(10), 1614–1624. Available from: https://doi.org/10.1016/j.cub.2019.04.027

Lehretz, G.G., **Sonnewald, S.** & **Sonnewald, U.** (2021) Assimilate highway to sink organs – physiological consequences of SP6A overexpression in transgenic potato (*Solanum tuberosum* L.). *Journal of Plant Physiology*, **266**, 153530. Available from: https://doi.org/10.1016/j.jplph.2021.153530

Livak, K.J. & **Schmittgen, T.D.** (2001) Analysis of relative gene expression data using real-time quantitative PCR amd the 2-ΔΔCT method. *Methods*, **25**(4), 402–408. Available from: https://doi.org/10.1006/meth.2001.1262

Martignago, D., **da Silveira Falavigna, V.**, **Coupland, G.** & **Conti, L.** (2025) Dancing molecules: group a bZIPS and PEBPs at the heart of plant development and stress responses. *Journal of Experimental Botany*. Available from: https://doi.org/10.1093/jxb/eraf034

Martin, A., **Adam, H.**, **Diaz-Mendoza, M.**, **Zurczak, M.**, **González-Schain, N.D.** & **Suárez-López, P.** (2009) Graft-transmissible induction of potato tuberization by the microRNA miR172. *Development*, **136**(17), 2873–2881. Available from: https://doi.org/10.1242/dev.031658

Miroshnichenko, D., **Firsov, A.**, **Timerbaev, V.**, **Kozlov, O.**, **Klementyeva, A.**, **Shaloiko, L.** ***et al.*** (2020) Evaluation of plant-derived promoters for constitutive and tissue-specific gene expression in potato. *Plants*, **9**(11), 1520. Available from: https://doi.org/10.3390/plants9111520

Murashige, T. & **Skoog, F.** (1962) A revised medium for rapid growth and bio assays with tobacco tissue cultures. *Physiologia Plantarum*, **15**, 473–497. Available from: https://doi.org/10.1111/j.1399-3054.1962.tb08052.x

Nicot, N., **Hausman, J.-F.**, **Hoffmann, L.** & **Evers, D.** (2005) Housekeeping gene selection for real-time RT-PCR normalization in potato during biotic and abiotic stress. *Journal of Experimental Botany*, **56**(421), 2907–2914. Available from: https://doi.org/10.1093/jxb/eri285

Oparka, K.J., **Roberts, A.G.**, **Boevink, P.**, **Santa Cruz, S.**, **Roberts, I.M.**, **Pradel, P.** ***et al.*** (1999) Simple, but not branched, plasmodesmata allow the nonspecific trafficking of proteins in developing tobacco leaves. *Cell*, **97**(6), 743–754. Available from: https://doi.org/10.1016/s0092-8674(00)80786-2

Park, J.-S., **Park, S.-J.**, **Kwon, S.-Y.**, **Shin, A.-Y.**, **Moon, K.-B.**, **Park, J.M.** ***et al.*** (2022) Temporally distinct regulatory pathways coordinate thermo-responsive storage organ formation in potato. *Cell Reports*, **38**(13), 110579. Available from: https://doi.org/10.1016/j.celrep.2022.110579

Patro, R., **Duggal, G.**, **Love, M.I.**, **Irizarry, R.A.** & **Kingsford, C.** (2017) Salmon provides fast and bias-aware quantification of transcript expression. *Nature Methods*, **14**(4), 417–419. Available from: https://doi.org/10.1038/nmeth.4197

Sakamoto, A., **Nishimura, T.**, **Miyaki, Y.**, **Watanabe, S.**, **Takagi, T.**, **Izumi, S.** ***et al.*** (2015) In vitro and in vivo evidence for oxalate oxidase activity of a germin-like protein from azalea. *Biochemical and Biophysical Research Communications*, **458**(3), 536–542. Available from: https://doi.org/10.1016/j.bbrc.2015.02.002

Sarrion-Perdigones, A., **Falconi, E.E.**, **Zandalinas, S.I.**, **Juárez, P.**, **Fernández-del-Carmen, A.**, **Granell, A.** ***et al.*** (2011) GoldenBraid: an iterative cloning system for standardized assembly of reusable genetic modules. *PLoS One*, **6**(7), e21622. Available from: https://doi.org/10.1371/journal.pone.0021622

Teo, C.J., **Takahashi, K.**, **Shimizu, K.**, **Shimamoto, K.** & **Taoka, K.I.** (2017) Potato tuber induction is regulated by interactions between components of a tuberigen complex. *Plant & Cell Physiology*, **58**(2), 365–374. Available from: https://doi.org/10.1093/pcp/pcw197

Viola, R., **Pelloux, J.**, **van der Ploeg, A.**, **Gillespie, T.**, **Marquis, N.**, **Roberts, A.G.** ***et al.*** (2007) Symplastic connection is required for bud outgrowth following dormancy in potato (*Solanum tuberosum* L.) tubers. *Plant, Cell & Environment*, **30**(8), 973–983. Available from: https://doi.org/10.1111/j.1365-3040.2007.01692.x

Viola, R., **Roberts, A.G.**, **Haupt, S.**, **Gazzani, S.**, **Hancock, R.D.**, **Marmiroli, N.** ***et al.*** (2001) Tuberization in potato involves a switch from apoplastic to symplastic phloem unloading. *Plant Cell*, **13**(2), 385–398. Available from: https://doi.org/10.1105/tpc.13.2.385

Woo, E.J., **Dunwell, J.M.**, **Goodenough, P.W.**, **Marvier, A.C.** & **Pickersgill, R.W.** (2000) Germin is a manganese containing homohexamer with oxalate oxidase and superoxide dismutase activities. *Nature Structural Biology*, **7**(11), 1036–1040. Available from: https://doi.org/10.1038/80954

Wright, K.M. & **Oparka, K.J.** (2006) The ER within plasmodesmata. In: Robinson, D.G. (Ed.) *The plant endoplasmic reticulum. Plant cell monographs*, Vol. **4**. Berlin, Heidelberg: Springer, pp. 279–308. Available from: https://doi.org/10.1007/7089_060

Zaynab, M., **Peng, J.**, **Sharif, Y.**, **Fatima, M.**, **Albaqami, M.**, **Al-Yahyai, R.** ***et al.*** (2022) Genome-wide identification and expression profiling of germin-like proteins reveal their role in regulating abiotic stress response in potato. *Frontiers in Plant Science*, **12**, 831140. Available from: https://doi.org/10.3389/fpls.2021.831140

Zhang, X., **Campbell, R.**, **Ducreux, L.J.M.**, **Morris, J.**, **Hedley, P.E.**, **Mellado-Ortega, E.** ***et al.*** (2020) TERMINAL FLOWER-1/CENTRORADIALIS inhibits tuberisation via protein interaction with the tuberigen activation complex. *The Plant Journal*, **103**(6), 2263–2278. Available from: https://doi.org/10.1111/tpj.14898

Zierer, W., **Rüscher, D.**, **Sonnewald, U.** & **Sonnewald, S.** (2021) Tuber and tuberous root development. *Annual Review of Plant Biology*, **72**, 551–580. Available from: https://doi.org/10.1146/annurev-arplant-080720-084456